

LARC 6DOF 3/3/00 [Yellow], Requiredmnvr exec errors  
& TCM4 Planning Ellipse [Green: LARC 3DOF 11/23/99]

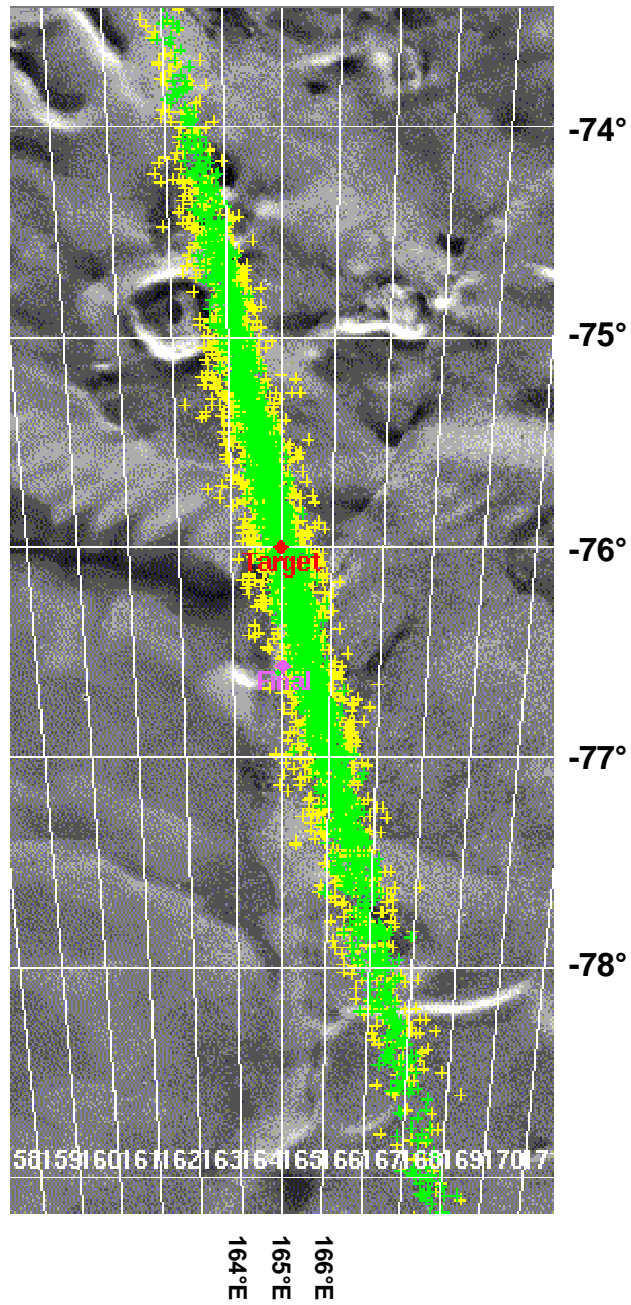
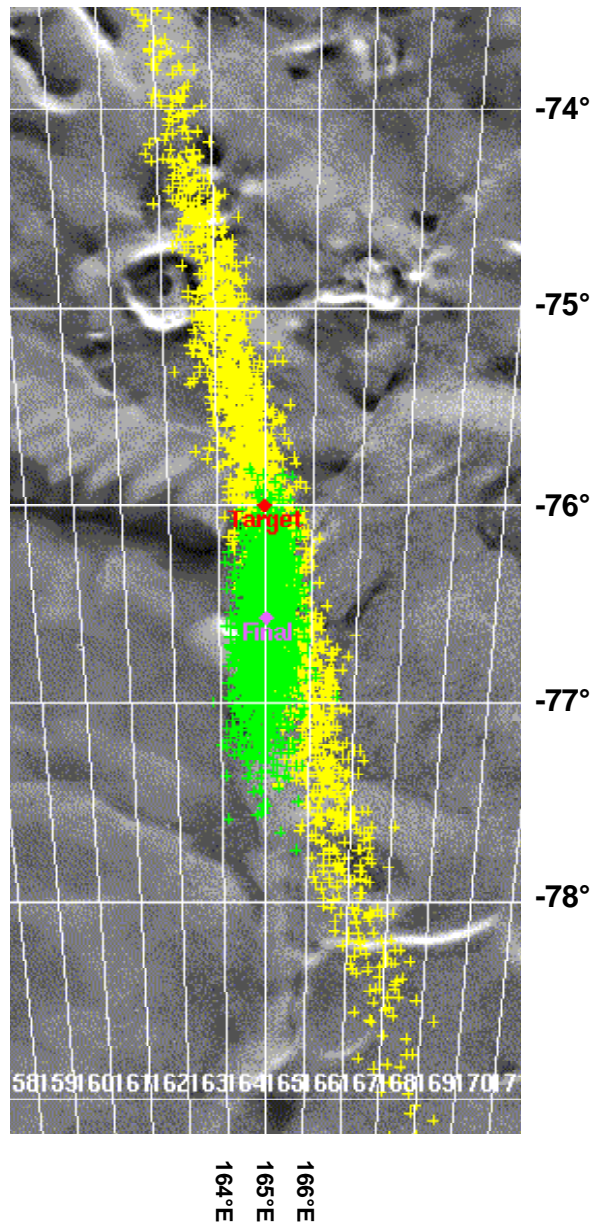


Figure 7-3. Required Maneuver-Execution Errors, LaRC 6DOF 3/3/00 (Yellow [Light]) and TCM-4 Planning Ellipse, LaRC 3DOF 11/23/99 (Green [Dark])

**LARC 6DOF 3/3/00 [Yellow], Requiredmivr exec errors  
& Final Estimate Ellipse [Green: LARC 6DOF 3/3/00]**



**Figure 7-4. Required Maneuver-Execution Errors, LaRC 6DOF 3/3/00 (Yellow [Light])  
and Final Estimated Ellipse, LARC 6DOF 3/3/00 (Green [Dark])**

Some concern has been expressed regarding how close the ultimate landing site was to a questionable terrain feature immediately to the west of the reconstructed landing site. Features equally hazardous appear further north on the western edge of the planned landing ellipse and on the eastern edge of the landing ellipse. These risks were known and accepted when the landing site was selected and did not represent risks that were higher than any alternative landing site during the early fall of 1999 at the time when a burn could have been executed to move the landing site. During the days prior to EDL, the cross-range drift (subsequently attributed to TCM-4 execution errors) was observed; however, as previously discussed, the project maneuver strategy did not allow for cross-track corrections at TCM-5.

Additionally, as discussed in the introduction to this section, questions have been raised during the post-EDL anomaly investigation regarding whether or not the expected control on center of mass was actually achieved in flight (see sections 7.5.3 through 7.5.5). In the extreme, if it is postulated that all fuel used during cruise might have been drawn from one tank or the other, rather than evenly from both, this would lead to motion of the center of mass of 12 millimeters, against the specification limit of 2.8 millimeters. This is not believed to be the case. There are in-flight data as late as TCM-5 showing that this probably had not happened. The potential for this effect is discussed further in Sections 7.5.3 through 7.5.5. Note that in the extreme northern case (12 millimeters motion of the center of mass, causing steep entry), simulations predict that the lander has a less than 19-percent chance of completing the parachute/propulsive descent before impact or touchdown.

#### PROCESS ASSESSMENT

The spacecraft design and the manner in which it was required to operate were not well suited to the levels of navigation accuracy that the project was attempting to achieve. The elements that follow necessitated a significant effort on behalf of the entire JPL navigation community to meet the demands of the mission's entry corridor:

1. Spacecraft operability issues — for example, an uncoupled thruster, which made the system much more susceptible to short-pulse modeling errors that were uncharacterized until late in cruise.
2. Post-launch anomalies — for example, Star Camera view-angle restrictions, which caused more frequent attitude/thruster disturbances.
3. Overly optimistic assumptions regarding the quality and obtainability of new unproven navigation data types — for example, near-simultaneous tracking.

The staff for the project navigation team originally planned prior to the loss of MCO would probably not have succeeded in meeting these entry conditions had they followed the pre-launch navigation plan while simultaneously conducting both MCO aerobraking and the MGS mapping mission.

#### LESSONS LEARNED

1. Increase the level of involvement of peers outside of the project in the future development of navigation plans and navigation requirements on the spacecraft and tracking systems.
2. Ensure that adequate attention is paid to spacecraft operability features (for example, coupled thrusters) if tight navigation control is required for the mission. Alternatively, if cost is the chief driver, accept larger accuracy errors by constraining landing site options.
3. Conduct in-flight validation of the assumed small-forces disturbance environment either with an early cruise calibration or via another onboard sensing technique (for example, appropriately scaled accelerometer, body-rate/impulse calibration).
4. Develop a maneuver strategy to ensure that all desired entry conditions are met (along-track and cross-track). This is less sensitive to unvalidated assumptions regarding the performance of either the spacecraft (small-forces frequency or accuracy, or maneuver-execution accuracy) or of new

tracking data types. Maintain sufficient resources during the operations phase so that, if necessary, the strategy can be revisited after launch once the assumptions have been validated or invalidated. Post-launch changes to the plan must be communicated expeditiously to all concerned parties via a formal change control process.

5. Maintain a level of control of the spacecraft center of mass — accounting for all sources — that is adequate to achieve precision landing site control.
6. Develop and institute a high-fidelity end-to-end EDL simulation capability during spacecraft development. Assign single-point responsibility for the development and application of this capability. Ensure proper interfaces between this simulation and the spacecraft and navigation teams. Update this simulation at several discrete points during operations but well prior to Mars arrival.

### 7.1.2 Heatshield Design or Physical Flaw

#### FAILURE MODE DESCRIPTION

The failure of the heatshield to protect the lander from the hypersonic atmospheric flow or to hold the lander's orientation during entry could result in catastrophic mission loss. The most credible source of heatshield failure is burnthrough as a result of a cavity created by the impact of a micrometeoroid.

#### FINDINGS

The MPL heatshield design, manufacturing, and verification methodology have a high degree of heritage to the successful Mars Pathfinder heatshield. An instrumentation package on board Mars Pathfinder provided significant design validation data in the Martian environment after the successful landing of that spacecraft. The environment for MPL is generally less stressing than that seen by Pathfinder, and the thickness of the thermal protection system (TPS) was correspondingly reduced.

#### PROCESS ASSESSMENT

One deviation from Mars Pathfinder heritage was noted: the inclusion of a tooling fixture hole in the support structure underlying the TPS. Earlier testing on Mars Pathfinder with unsealed holes demonstrated the possibility of burnthrough under such conditions. After the implications of this deviation were considered, the project completed arcjet testing to verify that the presence of this hole posed no EDL threat to MPL. A sample was prepared using the same manufacturing process as the flight article, which included "sealing" flow from the TPS through the hole with adhesive material. The arcjet testing was completed with no signs of TPS or heatshield compromise.

The cavity size created by a micrometeoroid impact in the heatshield material has not been quantified; however, in many materials the cavity size is approximately an order of magnitude larger than the micrometeoroid. The size of the cavity required to cause heatshield burnthrough is also unquantified, but is probably larger than in PICA heatshield material (this size is also uncertain; however, it appears to be approximately 6 millimeters). The combination of these uncertain (but in combination probably conservative) assumptions with the standard micrometeoroid flux model gives a failure probability of approximately 1 percent. Because micrometeoroid damage calculations seem to consistently overestimate damage probability, this 1-percent value can reasonably be considered an upper bound estimate, with a lower bound estimate approximately an order of magnitude smaller. A bumper shield would provide substantial protection against micrometeoroid impact; however, this has not been incorporated on past entry vehicle missions (Pioneer Venus, Galileo, Pathfinder) as a cost/benefit decision.

Overall, the Board concludes that the heatshield design contains substantial margins and that there are no indications of any significant opportunity for damage prior to EDL.

#### LESSONS LEARNED

The phenomenology of burnthrough in unsealed holes does not seem to be well understood. If future projects intend to fly TPS systems over support structures containing such discontinuities, additional testing should be conducted to ensure that the purported “sealing” mechanism does in fact adequately address this failure mode for surface discontinuities of the appropriate dimension.

The assessment as to whether or not a micrometeoroid bumper shield is warranted should be made on a project-by-project basis, with appropriate consideration for the overall Mars Program objectives, and taking into account not only the probability of catastrophic micrometeoroid impact damage, but the cost of loss of vehicle relative to the cost of such a bumper.

### **7.1.3 MPL Landing Site Unsurvivable**

#### FAILURE MODE DESCRIPTION

MPL was designed to survive landing site conditions incurring slopes of up to 10 degrees, with a load-bearing strength capable of ultimately imparting at least 222.5 N (50 lbf) to any of the three landing leg pads, and free of rocks or other obstacles taller than 35 centimeters. Terrain exceeding these limits could potentially overturn the lander or cause damage to the lander’s undersides or internal components. Additionally, the lander must control its azimuthal orientation on landing to achieve the desired orientation for maximal solar power and MGA articulation range of motion. Nominally, this is achieved by the control system prior to touchdown (to within an accuracy of 5 degrees). However, unforeseen conditions on the surface (for example, loose material at the surface covering a hard, frozen subsurface) could compromise this requirement, causing the lander to “spin out” on touchdown and come to rest in an orientation incapable of achieving MGA downlink on the first sol. This would prevent the lander from generating enough power to survive until the UHF contact attempt two sols later.

#### FINDINGS

The pre-launch test program appears to have adequately demonstrated that the lander could survive the specified landing conditions without damage to the structure and that the terrain would not result in the lander tipping over. Verification that azimuthal rotations will be achieved on touchdown was shown by analysis, not test, with certain surface properties assumed. Definitive statements regarding whether or not the specified landings were actually achieved at touchdown cannot be made.

The laser altimeter data from MGS indicate that the large-scale (100-meter footprint) slopes are much less than 10 degrees in the MPL landing ellipse. The exception is a large depression that covers 5 to 10 percent of the landing ellipse; this depression appears to contain slopes greater than 10 degrees. Furthermore, these data do not preclude the possible existence of steeper local slopes on the scale of the lander. Thermal-emission data from MGS also indicate that the surface of the landing site is covered with a material that has a low thermal inertia, typically indicative of loosely packed material. The thickness of this material cannot be definitively ascertained, although the MGS data suggest that it uniformly covers most of the surface to a depth of at least 1 centimeter. The presence of large rocks on the surface, which cannot be ruled out via the MGS imaging data, is deemed highly unlikely on the basis of remote-sensing thermal-inertia data.

## PROCESS ASSESSMENT

The validation of lander survivability, given all known data regarding the landing site, appears to have been adequate. The lander design relies upon achieving a preferred azimuth attitude orientation in order to generate adequate power for the entire mission. The MGA's limitations could also preclude immediate contact once on the surface.

## LESSONS LEARNED

On the basis of the intrinsic limitations of orbital remote-sensing data, the decision as to whether or not active hazard avoidance is warranted should be made on a project-by-project basis. Appropriate consideration should be given to the overall Mars Program objectives. The cost of the loss of vehicle relative to the cost of developing and qualifying such a system should also be considered.

The inclusion of a low-gain transmit antenna provides an added degree of robustness against the loss of communications due to spin out at touchdown. However, this does not provide protection against rotations large enough to compromise the lander's ability to maintain positive energy balance.

### **7.1.4 MPL Backshell/Parachute Recontacts or Drapes Over Lander After Touchdown**

#### FAILURE MODE DESCRIPTION

At approximately 1.2 kilometers above the surface of Mars, the lander determines that it is at an appropriate altitude (based on residual velocity) to begin its propulsive terminal descent and releases itself from the backshell/parachute assembly. If the backshell/parachute assembly comes to rest in close proximity to the lander after it has completed its propulsive descent to the surface, the lander may be damaged and unable to complete its mission. For example, the lander would not be able to deploy mechanisms such as the solar array, MGA, and the science masts/arms.

#### FINDINGS

Simulation of the descent of the backshell/parachute assembly — conducted independently by teams at NASA LaRC/JPL and LMA — indicate that it is possible, although not likely (<1-percent probability) that the backshell/parachute came to rest on the surface of Mars in close enough proximity to allow the parachute or its riggings to drape over the lander. The probability of the backshell structure itself recontacting the lander on the surface is considerably smaller (recontact prior to touchdown of the lander was also analyzed and shown to be implausible). The simulation shows that the timing of events is such that the backshell/parachute assembly would be on the ground and potentially draped over the lander prior to any of the deployments autonomously commanded by the lander.

#### PROCESS ASSESSMENT

The possibility of this occurring was not seriously considered or analyzed until after EDL. No analysis was performed to characterize the likelihood of such an event; therefore, no design modifications were considered to mitigate this failure mode.

#### LESSONS LEARNED

Future lander projects should consider some mechanism or maneuver to increase the horizontal separation distance between the landing sites of the lander and the parachute/backshell, if this can be done without increasing other mission risks to a probability higher than what has been identified for this mode.

## ***Bibliography***

Analysis of MGS/MOC Observations of the Mars Polar Lander (MPL) Landing Zone, Michael Malin, February 24, 2000, HTML Publication.

Analysis of MGS/MOC Observations of the Mars Polar Lander (MPL) Landing Zone — Supplementary Data, Michael Malin, March 7, 2000, HTML Publication.

CG Offset Effect on Landed Location — Willcockson and Wynn, January 26, 2000, viewgraph presentation to Environment and Landing Site Review Team at LMA, February 1, 2000.

Heatshield Review — Ron Turner, February 1, 2000, viewgraph presentation to Environment and Landing Site Review Team at LMA, February 1, 2000.

Heatshield Structure Pinhole Arc Jet Testing — Jan Thornton, February 1<sup>st</sup>, 2000, viewgraph presentation to Environment and Landing Site Review Team at LMA, February 1, 2000.

Lander/Backshell Recontact Analysis, MPL/DS2 Mishap Investigation — Spencer (JPL), Desai, and Queen (LaRC), February 1, 2000, viewgraph presentation to Environment and Landing Site Review Team at LMA, February 1, 2000.

MOC Photoclinometry — Mike Malin, 1/24/2000, viewgraph presentation to Environment and Landing Site Review Team at JPL, January 24, 2000.

MPL Area Analysis of Pulse Widths [from MGS MOLA] — Maria Zuber to Casani, Whetsel, Murray, and MacPherson, February 6, 2000, e-mail correspondence.

MPL Entry Risk Status Report — MacPherson et alia, November 19, 1999, viewgraph presentation to JPL MPL EDL Red Team.

MPL Lander to Backshell Clearance — Bill Willcockson, February 1, 2000, viewgraph presentation to Environment and Landing Site Review Team at LMA, February 1, 2000.

MPL Landing Estimates — Phil Knocke, January 13, 2000, viewgraph presentation to Environment and Landing Site Review Team at LMA, February 1, 2000.

MPL Maneuver Overview — Phil Knocke, January 13, 2000, viewgraph presentation to Environment and Landing Site Review Team at LMA, February 1, 2000.

MPL Small Forces Issues — Stu Spath, January 19<sup>th</sup>, 2000, viewgraph presentation to Environment and Landing Site Review Team at LMA, February 1, 2000.

MPL/DS2 Aero Environment Splinter, Entry Body Mass Properties — Kim Barnstable, February 1<sup>st</sup>, 2000, viewgraph presentation to Environment and Landing Site Review Team at LMA, February 1, 2000.

MPL/DS2 Review — Environment Review Team Session #1 Agenda — Charles Whetsel, January 24, 2000.

MPL/DS2 Review — Environment Review Team Session #2 Agenda — Charles Whetsel, February 1, 2000.

Presentation — MPL Aeroshell Environments and TPS Design, — Willcockson, Edquist, and Thornton, February 1, 2000, viewgraph presentation to Environment and Landing Site Review Team at LMA, February 1, 2000.

Re: Actions from 1/24 MPL/DS2 Landing Site Splinter, Ken Herkenhoff to Charles Whetsel, March 7, 2000, Email Correspondence.

Re: MPL Landing Site... [Absence of Terracing] — Tom Duxburry to Charles Whetsel, February 11, 2000, e-mail correspondence.

TCM-5 Rationale – Cross-track Capability — Phil Knocke, February 1, 2000, viewgraph presentation to Environment and Landing Site Review Team at LMA, February 1, 2000.

## 7.2 MPL Mechanical Systems

### INTRODUCTION

This section summarizes the failure mode examinations and findings of the Mechanical Systems Review Team. The reviews were conducted in two main parts: first, two full days of meetings with LMA mechanical systems engineers at Denver on 19–20 January 2000. The second was a 5-hour teleconference on 3 February to review follow-up actions produced from the 19–20 January meetings. Several additional teleconferences were held to cover various related subjects. Meetings and teleconferences were conducted with hardcopy presentation charts (see Bibliography).

### 7.2.1 Lander/Aeroshell Fails to Separate from Cruise Stage

#### FAILURE MODE DESCRIPTION

This failure results in the catastrophic entry and descent of the unseparated cruise stage and the lander/aeroshell. The following sub-failures lead to the primary failure:

- a) Release nut fails to release bolt. There are six release nuts at this interface. This failure can be caused by other specific failures in nut mechanical actuation, NSIs, pyro cabling, or pyro electronics.
- b) Push-off spring fails (broken spring). Insufficient separation spring force.
- c) Separation connector/ESD cover and/or other drag forces/energy exceeds separation spring forces/energy.
- d) Cold welding of aluminum-to-aluminum interfaces.
- e) Mechanical hang-up between separating hardware.

#### INTRODUCTION

The Mechanical Systems Review Team met with LMA engineering on 19 January 2000. Materials handed out at this meeting, as well as other materials gathered at subsequent meetings and via e-mail, are listed in the Bibliography. All the failure modes were examined. Follow-up actions were produced at this meeting and subsequently closed.

#### FINDINGS

The cruise stage separation simulation shows that, under stacked worst-case conditions, the separating rings may have one glancing contact during the first inch of separation travel. This contact occurs with one 50 percent failed push-off spring and maximum differential connector pull forces. In this case, separation is fully successful. LMA has analyzed the potential contact to ensure that this condition does not prevent separation. There is no hang-up. Connector pull forces used in the analysis were twice the magnitude of forces measured in connector qualification tests on MSP '98 and '01. Nominal separation conditions, which include worst-case differential connector pull forces, produced no contact between separating bodies. No condition was found that would prevent separation or damage hardware. Cruise stage separation velocity is 4 inches per second.

There is a momentary, small, negative force balance between connector pulls; however, the energy balance at this point is generous. The separation joint energy margin is 1.4. This momentary condition is judged to be acceptable.

There are six equally spaced release nuts and push-off springs at the flanged ring separation joint. Two diametrically opposite ITT Canon connectors are differentially lanyard-pulled at 0.3–0.6 inch and



0.5–0.8 inch of separation travel. There are also two hard-mounted RF connectors. The MPL ATLO system separation test verified that the connectors separate properly.

The release devices are 1/4-inch Hi-Shear nuts. These are highly reliable devices with substantial flight history. Lot acceptance and qualification tests of the devices were performed. The flight separation nuts were tested during the system-level deployment and separation tests. A release nut failure is unlikely. However, given that one of the release nuts failed to release its bolt, there is enough structural compliance to allow push-off springs to open the separating rings by the amount necessary to release at least one DS2 probe. Push-off springs were test verified for force and stroke during system-level separation tests. Springs were load tested and cycled at the component level.

Potential cold welding of the 2219-T851 chromate, conversion-coated aluminum surfaces at the separation interfaces was found not to be credible. Low compressive loads and conversion surface film prevent cold welding. An LMA materials expert made the presentation; the JPL materials expert was in agreement.

A system-level, quasi-static separation test was conducted over the full range of separation distance using live pyro firings and flight separation devices. These ATLO tests verified flight connector and spring forces, and separation clearances. There were no interferences or anomalies. Separation clearances open up quickly after the first inch of travel.

Margins for the separation system and its components are adequate.

#### PROCESS ASSESSMENT

The design, analysis, and verification process for this separation joint was more than adequate.

#### LESSONS LEARNED

For future designs, providing more radial clearance between the separating rings to avoid any possibility of glancing contact would be an improvement.

### **7.2.2 Center-of-Mass Migration Due to Mechanical Shifting**

#### FAILURE MODE DESCRIPTION

A lateral migration of center of mass beyond requirements produces mission-critical aeroshell entry dynamics: skip-out, too steep, excessive coning, etc. The question here is: Are there credible failure modes for mechanical displacement of hardware that could account for center-of-mass shifts large enough to produce apparent loss of mission? *Note:* Center-of-mass shift due to propellant migration was reviewed by the Propulsion and Thermal Review Team.

#### INTRODUCTION

The Mechanical Systems Review Team met with LMA engineering on 20 January to review this mode. LMA made the presentation; there were no follow-on actions.

#### FINDINGS

For significant center-of-mass migration due to mechanical shifting to take place, component structural failure and displacement must occur. Various hypothetical mass properties cases were examined and no credible scenario was found. All inserts were pull tested and structure was static tested. Center-of-mass uncertainty due to heatshield-to-backshell hole tolerances represents the largest

plausible mass moment shift. This uncertainty has already been accounted for in the mass properties predictions. No failures of this nature were evident during cruise.

#### PROCESS ASSESSMENT

The structural design, testing of the system, and mass properties analysis used in mitigating this failure mode were found to be acceptable.

### 7.2.3 Parachute Fails to Deploy and Inflate

#### FAILURE MODE DESCRIPTION

This failure can be caused by any of the following:

- a) Mortar fails to fire/deploy.
- b) Mortar cover fails to separate.
- c) Parachute fails to inflate.
- d) Parachute fails to sustain loads.

#### INTRODUCTION

The Mechanical Systems Review Team met with LMA engineering on 20 January to review this mode; LaRC participated via telephone. LMA made the presentation. All the failure modes were examined. Prior to this meeting, a parachute design consultant from NASA LaRC interviewed cognizant LMA engineers, and the report “Justification for Non-Standard Disk-Gap-Band (DGB) Parachute on Mars Pathfinder Project” (document ME-2589-Rpt., Rev. A) was reviewed.

#### FINDINGS

1. Mortar fails to fire/deploy — The mortar gas generator was qualified for Mars Pathfinder and MPL. It has dual NSIs and is a highly reliable system. The reliability of the gas generator and mortar to deploy the parachute is high. The energy margin provided by the gas generator to deploy the parachute is high.
2. Mortar cover fails to separate — The only difference between the MPL mortar system and the Mars Pathfinder mortar system is that from Mars Pathfinder to MPL the cover thermal protection was changed from Sirca to SLA-561. The mortar cover is held in place by three screws, which tear out when sufficient force is generated by the mortar deployment. The energy provided by the mortar deployment is several times that required to remove the cover and screws. This same mortar cover design has been deployed literally dozens of times without failure.
3. Parachute fails to inflate — The MPL parachute was a true heritage item from Mars Pathfinder. The only difference between the two parachutes was that the Mars Pathfinder logo was removed from the MPL chute.

The parachute is a disk-gap-band (DGB) design. The original Mars Pathfinder design was based on the Viking design, scaled down and modified. The modifications were made because the lateral oscillations of the Mars Pathfinder lander beneath the chute were considered to be unacceptable (up to 24 degrees) for the firing of the Mars Pathfinder rocket-assisted descent (RAD) rockets. The modification consisted of widening the band beneath the gap, which decreased the lateral oscillations to an acceptable level.

The deployment conditions for the MPL parachute are estimated to have been between M 1.7 and 1.85, and at a dynamic pressure of between 440 and 564 N/m<sup>2</sup>. It should be noted that the entry ballistic coefficients of the Mars Pathfinder and MPL configurations are almost identical (62 to 63).

Neither the Mars Pathfinder nor the MPL parachutes underwent any high-altitude supersonic deployment qualification tests. Such deployment qualification was done by similarity with the Viking design. Deployment Mach number was qualified by similarity up to M 2.3. A panel of parachute experts was surveyed to determine if any of these experts had reservations about using the modified DGB parachute, and what, if any, additional tests they would recommend. Three out of nine recommended high-altitude (supersonic) deployment tests either in flight or in a wind tunnel. This survey is documented in the report, "Justification for Non-Standard Disk-Gap-Band (DGB) Parachute on Mars Pathfinder Project," document ME-2589-Rpt., Rev. A, written by the Pioneer Corporation.

The Mars Pathfinder program did, in fact, perform a series of low-altitude, subsonic deployment tests, which were all successful. MPL also performed three successful deployment tests, including one at nearly five times the expected MPL deployment dynamic pressure of 2700 N/m<sup>2</sup>.

The packing and installation in the mortar canister was performed by the same individual that packed the Mars Pathfinder chute.

4. Failure of the parachute to sustain loads — As previously stated, the MPL parachute design was tested at approximately five times the MPL deployment dynamic pressure.

#### PROCESS ASSESSMENT

The design of the Mars Pathfinder/MPL parachute was acceptable. Regarding qualification testing, although the low-altitude, subsonic deployment tests were highly successful and qualified the parachute for dynamic pressure and snatch loads, uncertainty still exists regarding the supersonic deployment performance and stability of the parachute. The qualification program was lacking in this regard.

#### LESSONS LEARNED

There is a small chance, however unlikely, that the MPL parachute did not inflate properly due to supersonic inflation dynamics and failed to decelerate the lander. A more comprehensive qualification program using either analysis (CFD) or test (actual design configuration and expected supersonic deployment conditions) would reduce the risk of this type of failure.

It is recommended that future missions conduct representative flight qualification tests wherever possible, unless compelling analysis or modeling strongly convinces the program to do otherwise.

#### **7.2.4 Heatshield Fails to Separate from Backshell**

##### FAILURE MODE DESCRIPTION

This failure prevents the lander from separating from the backshell. A recontact of the heatshield with the lander/backshell causing critical damage to the lander, or preventing its subsequent separation from the backshell, is an associated failure mode. The following sub-failures lead to the primary failure:

- a) Release nut fails to release bolt. There are six release nuts at this interface. This failure can be caused by other specific failures in nut mechanical actuation, NSIs, pyro cabling, or pyro electronics. The Avionics and Flight Software Review Teams verified performances requirements for power.
- b) Separation springs fail to provide required separation force/energy (failed spring).
- c) “Stiction” forces of Furon foam between separating surfaces larger than modeled and prevent separation (see page 4.4.2-13 of Entry and Descent Separation Analyses and Tests, LMA document VR022).
- d) Simultaneity between the last two release nuts fired exceeded 20 milliseconds, causing structural failure/hang-up at the last attachment fitting. The Avionics and Flight Software/Sequencing Review Teams verified simultaneity.
- e) Aerodynamic coupling force and suction force between separating heatshield and backshell potentially larger than expected, or incorrectly modeled, allowing recontact of heatshield and subsequent critical damage to the lander (see page 4.4.2-11 and 4.4.2-13 of LMA document VR022).

## INTRODUCTION

The Mechanical Systems Review Team met with LMA engineering on 19 January 2000. LMA presented the material. All failure modes were presented and reviewed; follow-up actions were closed.

## FINDINGS

An analytic simulation model was used for verification of heatshield separation. MPL relied on the Mars Pathfinder engineering development unit (EDU) heatshield separation test and the correlated modeling approach. Stacked worst-case configuration of parameters was used in analysis (wind gust, one spring failed, maximum/minimum dynamic pressures, aerodynamic coupling, suction, and maximum stiction). Analysis showed that worst-case for separation of the heatshield occurs at minimum dynamic pressure. The net static force margin is 1.1. The analysis also shows no recontact. The separation model was checked by an independent analyst.

A system-level, first-motion heatshield separation test was not performed and the release nut NSIs were not fired. Although this test was planned to be performed along with all other system deployment tests, late concerns about possible damage to the fragile TPS, high confidence in separability of the joint, and reliance on the Mars Pathfinder EDU heatshield separation test resulted in this test being cancelled. To mitigate the loss of system-level verification, two things were done. First, a bench test of one of the six separation modules using all of the active separation components was successfully completed. This test imposed worst-case loads as boundary conditions. Second, the pyrotechnic circuits were checked for continuity. Since the NSIs were potted onto cabling pigtails, no pyrotechnic firing at the system level was done.

Deletion of the system-level, first-motion separation test compromised the verification process and was inconsistent with performing that test on every other deployable element. The generally accepted method for verification of separation joints is to perform a full-up, system-level, quasi-static separation test. Early attention to ground handling test support equipment and lander test configuration would have made this test deletion unnecessary.

The heatshield was easily installed and removed several times during MPL ATLO. This is a relatively uncomplicated separation joint, with generous clearances.

Stiction test results were conservatively applied to separation analysis. Furon foam configuration on the MPL heatshield was identical to Mars Pathfinder. Separation interface configuration and materials were identical to Mars Pathfinder. A stiction force eight times larger than the modeled value would have been required to prevent separation.

Twelve separation nuts were fired during lot acceptance. No live firings were conducted at system level. A component-level test of one separation nut/spring/fitting assembly was performed. The same release and push-off devices were used on Mars Pathfinder.

The hardware design was straightforward and the component verification process was acceptable. The separation analysis and margins were acceptable.

#### PROCESS ASSESSMENT

Deletion of the system-level, first-motion separation test compromised the test verification process. Otherwise, the separation system design and component verification process was well done.

#### LESSONS LEARNED

For future missions, perform a system-level, first-motion heatshield separation test.

### **7.2.5 Legs Fail to Deploy**

#### FAILURE MODE DESCRIPTION

This failure could result in the lander not surviving touchdown, or in the overturning of the lander and subsequent inoperability of the UHF antenna, MGA deployment and pointing, solar panel deployment, etc. Some of the failures causing the primary failure on any leg are:

- a) G&H release nut fails to release bolt.
- b) Leg or stabilizer deployment spring fails.
- c) Retarding forces/energy during leg and stabilizer extension are larger than available spring forces/energy (for instance, friction at temperature and aerodynamics).
- d) Leg or stabilizer latch fails to engage.
- e) Leg hardware was incorrectly disassembled/reassembled for final stow, thereby preventing deployment.
- f) Interference with adjacent hardware in stowed configuration prevents deployment.
- g) Deployed and latched leg does not carry design loads.

The Mechanical Systems Review Team met with LMA on 20 January. LMA engineers made the presentations. All failure modes were examined; follow-up actions have been closed.

#### FINDINGS — TOUCHDOWN SENSOR

A review of previous EDU testing showed that during development testing of the legs, two deployment tests were performed in which the touchdown sensors were monitored. During the test, no sensor triggering was observed on any of the three legs. The leg springs were redesigned to improve latching by increasing the deployment force. Following redesign, another deployment test was performed, during which two of the three legs triggered. See Section 7.7.2 for further details.

## FINDINGS — LEG DEPLOYMENT

EDU leg mechanical qualification testing was complete. Testing included drop tests, lateral loads, descent vibration, deployment and latching, touchdown sensor actuation, and overturning stability. Flight leg testing included static loads, thermal cycling, deployment and latching, touchdown sensor actuation, and overturning stability. Flight legs were successfully deployed at qualification cold temperature and under adverse gravitational loading of 0.7 g.

The flight legs were successfully deployed during MPL ATLO system test. This test included pyrotechnic firing of release devices and manual actuation of touchdown sensors. The worst-case deployment energy margin = 3.7. This margin is robust. Static test load factor was 1.1 times 35 g's. Structural elements showed positive margins. The design, analysis, and test verification process for the legs was found to be adequate.

Possible loading of the propulsion lines due to the potential stowed stabilizer strut to P-clamp grommet interference was evaluated when the issue was discovered at Kennedy Space Center. The evaluation determined that launch loading of the stabilizer could induce a deflection of the descent thruster feed manifold of 0.064 inch. The analysis included a load uncertainty factor of 1.25, and no compliance from thermal blankets or P-clamp grommet where interference was likely to occur. Applying all worst-case assumptions to the potential interference resulted in acceptable loading of the propulsion manifold and thruster feed tubing. This potential interference is in a configuration that would not impede deployment of the stabilizer.

## PROCESS ASSESSMENT

The touchdown sensor spurious signal was a known characteristic of leg deployment. The design and verification process for the touchdown sensor was satisfactory.

There are no concerns relative to the successful deployment of legs, the actuation of the touchdown sensors, or the ability to withstand the design landing loads and stability. The design is satisfactory and has adequate margins. The design verification process is acceptable.

## LESSONS LEARNED

Electrical interfaces between mechanical and electrical sensors and software must be specified and controlled as part of the system design process.

### **7.2.6 Lander Fails to Separate from Backshell**

#### FAILURE MODE DESCRIPTION

This failure would result in the lander/backshell crashing on the surface. The following sub-failures can lead to the primary failure:

- a) The two release nuts adjacent to the guide rails are fired before the release nuts at the other two locations; i.e., firing sequence is backwards.
- b) The simultaneity between firing the last two nuts at the guide rails exceeds the 10-millisecond requirement.  
*Note:* Failures a) and b) can result in large loads at the guide rails, which would retard separation.
- c) Release nut fails to release bolt. There are four release nuts at this interface. This failure can be produced by other failures: nut does not actuate, NSIs fail to provide required energy, electrical pyro cabling is damaged, and pyro electronics fail to meet power requirements.
- d) Push-off springs fail to provide the required separation force/energy (failed spring).

- e) Separation connector drag forces are high enough to prevent separation.
- f) Friction coefficient between sliding backshell guide rod and lander guide tube was unconservatively determined or modeled. Degraded condition of guide rail surfaces produces retarding forces, which prevent separation.
- g) Cold welding between interfacing surfaces prevents separation.
- h) Larger than predicted bending moments and deflections applied to guide rails during separation result in retarding forces high enough to prevent separation; separation model parameters were unconservatively defined and/or modeled.
- i) Interference during separation between backshell and lander, caused by larger than predicted lateral shear deflection and/or angular tip-off rotation, prevents separation. Separation model parameters unconservatively defined and/or modeled.

## INTRODUCTION

The Mechanical Systems Review Team met with LMA on 19 January 2000. LMA engineers made the presentations. All the failure modes were examined; follow-up actions have been closed.

LMA identified and presented the following additional sub-failure mode: The Framotome lander separation connector lanyard fails due to higher than expected connector pull forces, or less than expected lanyard load capability. The connectors would be pulled apart in this case by the extended backshell connector cabling. The lander could be beyond guide rail engagement when the anomalous disconnects occur. This would cause higher than predicted retarding forces and higher than predicted transverse angular tip-off rates.

## FINDINGS

The proof test data for the Framotome connector lanyard were not available to verify lanyard capability. As a result of the review action, LMA completed lanyard proof tests and extensive connector pull force tests at ambient and predicted cold temperature. Test results showed acceptable lanyard strength margins and upper bound connector pull forces.

Framotome connector separation pull tests for the MSP '01 project, performed at  $-100$  degrees C, produced significantly larger separation forces than were measured in the MSP '98 Framotome connector pull tests. The MSP '01 project Framotome test results, with a generous factor of two, have been applied to the MPL lander separation analysis. The initial MPL tests did not adequately measure connector pull force and, therefore, did not verify the design function.

On 5 February 2000, the separation analysis was updated to include the current upper bound estimate of Framotome and Canon connector pull forces. Even with larger than expected connector pull forces or a Framotome lanyard failure, the large net force and energy margins make failure to separate the lander unlikely.

The absence of a Framotome lanyard proof test or other bounding analyses and the subsequent establishment of lanyard pull-force margin compromised the pre-launch design verification process.

The guide rails are used to align the separating bodies during the first 11 inches of separation travel. The design required these to prevent contact between close-proximity hardware. EDU quasi-static separation tests verified guide rail performance parameters, including moments and friction. Guide rail tests used the design requirement for parachute angle to backshell of 6 degrees, as compared to the nominal estimate of 2.5 degrees. The test set-up was fixed rather than free-free. This is conservative and would produce larger induced moments than could be expected in flight.

Analytic model simulation was used to verify separation under worst-case conditions. The model used test verified push-off spring forces, connector drag forces, REM seal disconnect forces, and guide rail moments. The analysis methods used in verifying the dynamic separation were acceptable and conservative.

A flight system-level quasi-static separation test was successfully performed using live pyro release nut firings, push-off springs, separation connectors/lanyards, and REM seals, over the full distance of guide rail engagement. Force versus displacement measurements were taken throughout the separation travel. Predicted minimum clearances were visually verified.

There are large separation force and energy margins. A factor of three times the conservatively modeled retarding forces is required to stop separation. High margin is due primarily to the work of Mars gravity.

Separation nuts and push-off springs (four each) are high-reliability components and were adequately qualified.

#### PROCESS ASSESSMENT

The verification process for validating the Framotome connector pull force and lanyard capability was not satisfactory.

The lander separation system is considerably more complex than either the cruise stage or backshell systems. The lander separation system was well designed. Large separation force and energy margins ensure separation. With the exception of the initial Framotome connector force and lanyard proof test verification issues, the verification process for the separation system was satisfactory.

#### LESSONS LEARNED

Connector pull-force tests at cold conditions should be conducted with fully configured connectors. Include proof test requirements for connector lanyards in vendor specifications, or verify lander performance during qualification tests.

### **7.2.7 Propulsion Dynamics Interaction with Structure**

#### FAILURE MODE DESCRIPTION

Rupture of propellant lines feeding the descent engines is a potential failure mode. It could be caused by water hammer forces interacting with propellant-line structural supports of insufficient stiffness to prevent excessive deflection of the lines. Excessive deflection of lines produces bending stresses in lines and fittings which, when added to propellant pressure stresses, could cause rupture. (See also Section 7.5.10.)

#### INTRODUCTION

The Mechanical Systems and Propulsion and Thermal Review Teams jointly met with LMA on 20 January 2000. LMA engineering presented the materials; follow-up actions were closed.



## FINDINGS

The descent engine cluster structural attachment to the spacecraft was acceptably designed and analyzed, with adequate margins.

Late changes in the descent engine duty cycle increased the dynamic interaction with the propellant tubing support system. This produced larger deflections and bending stresses in the tubing than the system had been designed and built for. This condition was addressed and resolved while the flight spacecraft was being prepared for launch at Kennedy Space Center.

The propulsion feed tubing material is 321 annealed stainless steel, a ductile material with good fatigue properties. It work-hardens and is weldable. Tubing is supported by elastomer lined clamps attached to fiberglass thermal isolation brackets. These brackets are attached to the core structure. Strength margins on the support system are satisfactory.

A test-correlated finite-element model (FEM) was used to analyze and predict dynamic loads in the tubing. The model was driven with the worst-case propellant pressure transients. A 1.25 model uncertainty factor was applied to the resulting loads. Damping used in the analysis was conservative relative to the flight installation. A comparison between the approximate method used for the MSP '98 analysis and a more accurate coupled structure fluid analysis showed the approximate method to be conservative in terms of both peak loading and number of cycles.

The model predicted yielding of material at two locations. The minimum ultimate strength margin of safety was positive. A worst-case fatigue analysis was performed at critical welds and showed positive margins above the required four lifetimes of cumulative fatigue effects. All stress concentration factors were applied. Eight weld specimens were dynamically tested with applied reversible bending moments and worst-case mismatch at welds. These data were used in conjunction with other applicable fatigue analysis data.

The configuration of the support system was satisfactory. The support system design stiffness was marginally adequate to handle the final water hammer loads. In this case, robustness at the early phase of the design would have more easily accommodated late developing increases in loads.

## PROCESS ASSESSMENT

The propellant lines have the capability to withstand the imposed stresses. The analytic process used to determine loads and validate the propellant line and structural system integrity was conservative and satisfactory.

## LESSONS LEARNED

Provide adequate design margin in the propellant line structural support system for all operating conditions.

### **7.2.8 Landed Solar Array Fails to Deploy**

#### FAILURE MODE DESCRIPTION

Failure to deploy the solar panel adjacent to the MGA would prevent the MGA from scanning. Articulation of the MGA with a stowed panel would probably result in severe damage to the feed and fragile graphite epoxy (Gr/E) antenna. The sub-failures are:

- a) Release nut fails to release bolt. There are two release nuts for each panel deployment. This condition can be produced by non-actuation of the mechanical elements of the nut, damaged cabling, and insufficient power from the electrical system.
- b) Deployment springs have insufficient force to rotate panel center of mass upward to over center deployment position (spring failure).
- c) Blocking of elastomeric material used as deflection limiters between stowed panel faces produces stiction forces large enough to prevent deployment.
- d) Power cabling service loop over hinge line produces sufficient retarding torque to prevent deployment.

#### INTRODUCTION

The Mechanical Systems Review Team met with LMA engineering on 20 January 2000. LMA made the presentation. All the failure modes were examined; there were no follow-up actions.

#### FINDINGS

The hinge-line monoballs were satisfactorily shielded from surface contamination with felt seals. Several well-simulated, ambient panel deployment tests were conducted. Thermal–vacuum deployment tests were performed with worst-case spring and gravity conditions. Hinge-line deployment torque margins were measured.

Flight system-level solar array deployment tests, including actuation of burnwire release devices, were successfully performed. Qualification and acceptance tests were performed on all mechanical devices. There is no stiction at Furon deflection limiters. The Furon interface surface is separated by Teflon. No contact pressure exists except intermittently during launch. The deployment hardware designs were found to be robust. Deployment margins were adequate. The verification process was complete.

#### PROCESS ASSESSMENT

The design, analysis, and test verification process was fully acceptable.

### **7.2.9 MGA Fails to Deploy**

#### FAILURE MODE DESCRIPTION

A failure of the MGA to deploy could result in the loss of telecommunications signal. This could occur if the stowed MGA fails to unlatch or if the two-axis gimbal system fails to articulate.

#### INTRODUCTION

The Mechanical Systems Review Team met with LMA via teleconference on 3 February to examine this mode. LMA presented the material. There were no follow-up actions.

#### FINDINGS

The gimbal had a redundant and cross-strapped optic encoder, and redundant stepper motor windings. Qualification-level random vibration, static load, and stiffness tests were performed on an EDU two-axis gimbal (TAG). EDU thermal–vacuum and 14× life tests were performed. A protoflight-level random vibration test was performed on the MGA TAG. The MPL ATLO system-level unlatch and full range-of-motion test was performed on the release device and the MGA TAG. There are generous torque margins over the beginning and end of life. Lot acceptance tests of the G&H separation nut

were satisfactory. The same MGA gimbal was used on the MSP '98 Mars Climate Orbiter solar array, with no cruise anomalies.

#### PROCESS ASSESSMENT

The MGA mechanical system design and test verification process was fully acceptable. The functional margins are high.

#### SUMMARY

The LMA mechanical systems designs were very well executed and verified, and the LMA team was highly experienced and motivated. The quality of the mechanical system-level integration of the spacecraft was outstanding.

The design review process was too hurried to allow LMA engineers sufficient time to reflect on their designs and prepare presentation materials. Also, there was insufficient time for the reviewers to absorb and penetrate the design. During the development process, peer reviews that focused on specific problem areas were very effective.

#### ***Bibliography***

Entry and Descent Separation Analyses and Tests, LMA document VR022, Lowell Coghurn, 10 December 1998.

Justification for Non-Standard Disk-Gap-Band (DGB) Parachute on Mars Pathfinder Project, document ME-2589-Rpt, Rev. A.

Legs Sensor, 24 February 2000, e-mail message from Lad Curtis.

LMA Comments on MPL/DS2 Loss Review Board report, e-mail from Lad Curtis, to John Casani, 2/15/00.

Mars Polar Lander Premature Descent Engine Termination Due to Touchdown (TD) Indication Conclusions, LMA charts, H. H. Curtis, R. Gehling, J. Bene, G. Bollendonk, February 25, 2000.

Mars Polar Lander Touchdown Sensor Code Issue, LMA charts, H. Curtis, January 20, 2000.

Mechanical Failure Review Splinter — Action Item Review handout package, February 3, 2000.

Mechanical Failure Review Splinter handout package, January 18–19, 2000.

TD Sensor PIE and Involvement, 25 February 2000, e-mail message from Lad Curtis.

## 7.3 MPL Dynamics and Control

### INTRODUCTION

The Dynamics and Control Review Team conducted a careful review of the MPL control system, including hardware elements, algorithms, sequences, software implementations, analyses, and testing. In support of the review process, a number of meetings, presentations, and analyses were performed. The documentation presented and used in the evaluations is listed in the Bibliography. Most items reviewed have been found sufficiently robust that they are considered to be “implausible” contributors to the loss of MPL. However, 11 items were found to require further study, either because of their importance to the EDL sequence, or because of the uncertainty in design margins. The following 11 items are discussed in detail in this section:

- Radar Data Lockout
- Radar–Terrain Interaction
- Inertial Measurement Unit (IMU) Performance
- Model Fidelity
- Inadequate Stability Margins
- Fuel Slosh
- Center-of-Mass Migration/Uncertainty
- Flexible Body Interactions
- Zero Velocity Singularity
- Margin at Minimum Thrust
- Radar–Heatshield Lockup

It was noted that a number of items were not truly failure modes per se, but could lead to effects that result in failure, and are therefore included in the list. These are Model Fidelity, Fuel Slosh, Center-of-Mass Migration/Uncertainty (including nonlinear effects and mixing logic), and Flexible Body Interactions. It is important to note that most of these items were considered by themselves to be an unlikely cause of the loss of MPL. However, a concern exists that the combined effects of the nonlinear pulse-width modulation, fuel slosh, mixing logic, propulsion dynamics (water hammer), etc., each contribute to the erosion of stability margins, and that the true stability margins are unknown.

#### 7.3.1 Radar Data Lockout

##### FAILURE MODE DESCRIPTION

In this potential failure mode, the Radar Doppler velocity measurements are never used and the system fails to achieve the required low landing velocity at touchdown.

A Mars-relative velocity estimate is initialized before entry and propagated using IMU measurements throughout entry and descent. The first Radar velocity measurement must be within a predetermined threshold of the IMU-propagated estimate or the Radar measurement will be rejected. This test is needed to prevent acceptance of bad Radar measurements. If the IMU estimate has a very large error, however, all Radar measurements will be rejected.

##### FINDINGS

During pre-launch design and verification, this failure was mitigated by the IMU calibration performed by the manufacturer and verified by the system contractor.

In-flight verification included cruise TCMs and reorientation maneuvers that were performed successfully throughout cruise. This gives a level of confidence that both the accelerometer and gyro modules of the IMU were operating well, though the available data are insufficient to re-verify all alignments and scale factors.

Frequent star update periods in cruise after tens of hours with no stars allow in-flight gyro bias and bias drift calibrations. These exonerate bias drift as a problem unless there was a gyro failure after the final star calibration.

This possible failure mode was investigated extensively in the month prior to Mars entry by the project and the Red Team. As a result of the investigation, the threshold was loosened to decrease the probability of this failure mode causing a problem. The threshold as set is loose enough that, for an IMU performing within specifications, the likelihood of such large IMU propagation errors is statistically remote. This failure mode requires IMU hardware operating significantly out of specification or unexpectedly harsh entry environments.

#### PROCESS ASSESSMENT

There is no logic in the software that takes corrective action in the event of continuous rejection of Radar measurements. This would have made the design more robust.

#### LESSONS LEARNED

Use of single measurements can lead to Radar data rejection. Multiple self-consistent Radar velocity measurements should be required before presenting a measurement for comparison with the IMU-propagated velocity estimate.

Added logic to the software could provide corrective action to eliminate the possibility of continuous rejection of Radar velocity measurements.

### **7.3.2 Radar-Terrain Interaction**

#### FAILURE MODE DESCRIPTION

In this potential failure mode, Radar measurement of sloped terrain produces a biased horizontal velocity measurement. This measurement error can produce horizontal velocities at touchdown that exceed the specification.

#### FINDINGS

The MPL Radar design makes use of broad radar beams. Based on the measured altitude, the Radar sets narrow time gates on the return pulse and assumes that the direction of the return is that corresponding to flat, level terrain. The actual measurements may be thought of as being made in a coordinate system with a vertical axis perpendicular to the plane of the measured surface. The attitude of this measurement coordinate system is unknown, hence the measurement error.

#### PROCESS ASSESSMENT

This effect was discovered about a month before landing and the simulations were corrected to demonstrate it. For the MPL system design (including the specifics of Radar measurement cutoff altitude and transition to constant velocity descent), the bias at touchdown is approximately 0.2 meter per second horizontal velocity for each degree of slope at Radar cutoff. This gives 2 meters per second for 10-degree slopes. This effect occurs in regions of slope of large (>50 meters) extent. Pre-launch

simulations attempted to include slope effects on Radar measurements, but the implementation was in error such that these effects were not observable in the simulations.

#### LESSONS LEARNED

Landing areas of small slopes or lower vertical velocity at Radar cutoff should be chosen. This may be accomplished by lowering the Radar cutoff altitude or raising the altitude of transition to constant velocity.

A Radar that does not have vulnerability to landing area slopes should be selected. For example, the Viking lander Radar used small beams, knew which direction the returns came from, and so was able to construct the velocity measurement in the lander reference frame. Another possibility is to study the feasibility of augmenting the NAV filter to be more robust to horizontal velocity errors due to the effect of landing site slope.

### 7.3.3 Inertial Measurement Unit (IMU) Performance

#### FAILURE MODE DESCRIPTION

Failure of the IMU to meet the performance requirements results in degraded terminal descent control.

The IMU provides the Guidance and Control System measurements of three axes “total angle” and velocity. From Guidance System initialization at L –15.5 minutes, the IMU performance requirements are:

- Attitude accuracy (per axis) — 0.15 degree, initialization to touchdown (1.5 hours duration from last calibration). Some reduction in accuracy is allowable after entry.
- Velocity accuracy (per axis) — 20 meters per second (from 6000 meters per second) until “Data Validity Check” is made with Radar velocity estimate.

The IMU-propagated attitude affects Radar-determined velocity. The IMU-propagated velocity is mixed with the Radar-determined velocity after acceptance of the Radar data, which are critical to terminal descent control requirements of 2.4 meters per second, vertical, and 1.4 meters per second, horizontal.

#### FINDINGS

Two units, provided by Honeywell, were launched on MPL. The supplier performed all the inertial instrument quality testing. The performance figures are described in Honeywell document 596-18884R. This is an exceptional IMU. Performance described is within the requirements of the MPL Attitude Control System.

Both units have been used in flight — one at a time, through launch and cruise. The A unit was selected for most of the cruise phase and EDL. Because of the 0.15-degree-per-axis attitude determination requirement, the last IMU calibration sequence using the Star Camera was performed and completed, as planned, 1.5 hours before touchdown. All spacecraft attitude maneuvers and TCMs utilized the IMU for attitude and velocity control and all were successful. All were performed under quiescent conditions. No in-flight calibration of gyroscope scale factor or accelerometer scale factor was performed. Supplier performance data were used.

## PROCESS ASSESSMENT

Based on the available documentation, it is believed that the projected performance of this IMU is excellent. The IMU was an excellent selection, well-suited to the task at hand.

## LESSONS LEARNED

The IMU calibration update process could be improved by correcting the stray light interference of the Star Camera. This allows IMU calibration without performing turns.

### **7.3.4 Model Fidelity**

#### FAILURE MODE DESCRIPTION

Incomplete and/or incorrect modeling of the spacecraft and/or of the Mars environment could have resulted in an inaccurate assessment of EDL system performance and of safety margins, which may have been below what is required for a successful landing.

#### FINDINGS

The MPL team understood the importance of modeling during the design, validation, and testing phases of EDL development, and considerable project resources were used in developing models of different degrees of fidelity and for different testbed environments. These models were incorporated into a Monte Carlo time simulation that becomes the main tool to assess system performance over a large range of system uncertainties.

This large modeling effort, however, may have not been enough to ensure success given the choice in the design phase of some of the system components, such as the propulsion system and the landing Radar, and given some aspects of the design of the Guidance and Control (G&C) algorithms/software, which resulted in a system that was extremely difficult to model and more sensitive to model errors than it might have been. The choice of pulse-width modulation (PWM) for controlling the thrust of the descent engines, while conceptually simple, presented a tremendous modeling challenge that the MPL team responded to with one of the most comprehensive water-hammer modeling efforts in the industry. While the quality of the work involved in this effort was outstanding and the resources invested considerable, it may have not been enough. The complexity of the interactions between the feed system, the thrusters, the structure, the G&C sensors, and the G&C algorithms that the PWM approach creates, practically dictate that the only way of verifying the system with high confidence is with a full-scale closed-loop test of the system. This test was prohibitive from a cost and schedule point of view and it was not done.

In addition, the choice of landing Radar with its broad beams resulted in a system whose performance is affected by the topography of the landing site and the spacecraft attitude, thus requiring for verification a very complex model of the Radar beams and of the Mars surface. The MPL team did not properly understand the technical issues associated with this surface interaction and as a result they used an incorrect model to test the system (see Section 7.3.2). Other aspects of the landing Radar, however, were extensively and properly modeled.

## PROCESS ASSESSMENT

While the modeling effort was perhaps not good enough to determine system margins and ensure mission success, the problem lies more with the hardware choices made early in the program, which resulted in a system that was extremely difficult to model and very sensitive to modeling errors, rather than with the commitment and the resources that the MPL team assigned to system modeling. In

addition, the rigid allocation for attitude control torques of 10 milliseconds out of 100 limited the robustness of the Attitude Control System (ACS).

#### LESSONS LEARNED

A full-configuration, closed-loop firing of the descent engines should be performed — or at the very least, a static test should be performed using all the engines firing pulse trains consistent with EDL powered descent. In addition, an extensive model of the landing Radar that properly models the interactions with the terrain should be developed and validated with additional drop tests. Finally, the G&C algorithms should be modified to make the system more robust to modeling errors, in particular in the area of landing Radar data validation, capability to handle unmodeled center-of-mass offsets, parachute dynamics, etc.

During component selection system, engineers should consider the effort and feasibility required to model a particular component as an extremely important criteria in the selection.

### **7.3.5 Unstable Limit-Cycle Behavior During Terminal Descent**

#### FAILURE MODE DESCRIPTION

This potential failure mode could have resulted from inadequate stability margins due to lack of nonlinear element characterization.

#### FINDINGS

LMA used “Flowtran” modeling for water hammer, which they correlated with hardware tests (including hot firings). Furthermore, the actual flight code and timing was used for the descent controller. There is no reason to suspect that the simulations performed did not reflect the actual performance of this nonlinear path. It is also probable that the Monte Carlo runs flooded the parameter and timing space.

#### PROCESS ASSESSMENT

This type of controller must exhibit limit cycle behavior and there was no analytical assessment of its magnitude nor whether the system might “fall off a cliff” to a large magnitude cycle. There is absolutely no evidence of such behavior and such behavior is not suspected, but a nonlinear analysis would yield increased confidence. The MPL descent control loop is very complex and nonlinear. There are few analytical tools to help in assessing the likelihood of unstable limit cycling occurring in such a controller, and the final arbiter must be the highest fidelity simulation possible. One of the key nonlinear paths in the controller is from desired torque to the actual applied torque. This path involves mixing logic with possible saturation, the PWM scheme, the thruster characteristics (including mount flexibility), and water hammer effects.

#### LESSONS LEARNED

The mathematical technique of harmonic balance has long been used in the analysis of nonlinear systems, e.g., Krylov–Bogoliubov (1934), and is applicable to the desired torque to actual torque nonlinearity. The Describing Function (Kochenburger) technique could be used to characterize this nonlinearity. This should prove useful for future margin assessment.

This technique will not address interactions due to the large amount of energy generated at the PWM frequency, its harmonics, and, with water hammer delays, possibly subharmonics. Nonlinear effects, such as rectification, could possibly translate this energy into sensing within the controller baseband.



The only certain way to eliminate control problems, to say nothing of the other effects of water hammer, etc., is to use a throttle control on the engines. Margins for throttle control are easily assessed and full-range control may be utilized with little complexity.

### **7.3.6 Fuel Slosh**

#### FAILURE MODE DESCRIPTION

In this potential failure mode, the pulse-mode descent thruster control excites propellant slosh modes in a way that erodes the stability margin of the control system.

#### FINDINGS

Propellant slosh was not simulated in the design of terminal descent control. Propellant slosh models were developed for use during cruise, but they are not applicable for terminal descent analysis.

#### PROCESS ASSESSMENT

The modeling that has been done does not rule out the possibility that slosh modes might be at frequencies that could be significantly excited by the 10-Hz, pulsed-mode descent thruster operation. Propellant slosh was not sufficiently addressed during the design to determine its effects on margin erosion. Analyses were performed on the free-tank case, but there was no extrapolation to the diaphragm case for EDL.

#### LESSONS LEARNED

Model the slosh dynamics in the presence of the diaphragm (supported by test) and assess any control system margin degradation.

### **7.3.7 Center-of-Mass Migration/Uncertainty**

#### **7.3.7.1 Cruise Phase Center-of-Mass Migration**

#### FAILURE MODE DESCRIPTION

This potential failure mode results in an angle of attack that is greater than 1 degree during entry if the cruise phase center-of-mass migration is greater than 2.8 millimeters from the design requirement location. Much larger angles of attack ( $>2\times$ ) could result in atmospheric skip-out, auger-in, or more benignly, large cross-range landing errors.

#### FINDINGS

Spin balancing of the spacecraft in launch configuration and of the cruise stage was performed. The entry module center of mass was verified by subtracting the cruise stage from launch configuration results.

TCM telemetry was analyzed and, although significant uncertainties still exist, bounds the cruise module center of mass to within 0 millimeter  $\pm 3.6$  millimeters, indicating that propellant migration was within expectation.

## PROCESS ASSESSMENT

The process to ensure that the center-of-mass requirement was met relied on two major components:

1. Pre-flight spin balancing.
2. A propulsion system design that would restrict differential propellant flow between the two propellant tanks during cruise to negligible levels.

Component 1 is accepted practice. Component 2 may not have been valid, since it seems to have been based only on analysis/engineering judgment. (See Section 7.5.4 for details.)

## LESSONS LEARNED

Reliance on the Propulsion Subsystem in meeting design requirements critical to attitude control should be verified by testing, if possible. (See Section 7.5.4 for details.)

### 7.3.7.2 Landing Phase Center-of-Mass Migration

#### FAILURE MODE DESCRIPTION

This potential failure mode could result from propellant migration prior to and during terminal descent. If the center of mass is more than 22.9 millimeters from the design requirement location, a large moment imbalance generated by 68-percent nominal duty cycle of symmetrically placed descent engines would result. Larger offsets could result in loss of attitude control authority due to exceeding the allocated  $\pm 10$  percent ( $\pm 10$  milliseconds) off-pulsing budgeted for attitude control.

#### FINDINGS

The lander center-of-mass requirement was met through a combination of analysis and the spin balance results of the cruise stage. Cruise module spin balance results imply lander center of mass to be within expectations, given that lander analysis is correct. However, significant propellant migration during descent is an unaccounted for possibility.

#### PROCESS ASSESSMENT

Allocation of control authority margins relative to center-of-mass requirements was inadequate with respect to accepted practice. This can be attributed largely to unsubstantiated confidence in the design of the propulsion system with respect to limiting the amount of propellant migration. See Section 7.5.7 for further discussion of the propellant migration issue.

#### LESSONS LEARNED

Reliance on the Propulsion Subsystem in meeting design requirements critical to attitude control should be verified by testing, if possible. See Section 7.5.7 for details.

Consideration should be given to designing a more robust control system. In particular, transient behaviors that can temporarily absorb control authority margins should be considered when allocating margins. Such events can include large dynamic disturbances injected into the control system due to mode-switching or events occurring at certain phases of the descent.

### 7.3.8 Adverse Flexible Body Interaction with Terminal Descent Controller

#### FAILURE MODE DESCRIPTION

This potential failure mode could result from flexing of the lander structure (excluding propellant slosh, which is covered elsewhere), causing an instability or large errors to accrue by interacting with the control system. Historically, these types of interactions have caused many problems.

#### FINDINGS

MPL, in the descent configuration (legs deployed), was modeled by LMA using a finite-element model in NASTRAN format. The NASTRAN output for free-free modes up to 100 Hz shows that the lander is very stiff with the lowest mode around 78 Hz and this mode only involves a solar panel in an “appendage” mode, not an “in-the-loop” flexibility. Such a cursory inspection indicates immediately that the gain stabilization of the loop along with the anti-aliasing filters would eliminate flexibility as a problem.

The University of Southern California was contracted to study the NASTRAN data and construct a simulation containing the lower 104 frequency modes. The study concluded that “Linear analysis based on the rigid spacecraft model is adequate for this case” and “flexibility does not cause limit cycling.”

The simulation developed in the course of this study (Simulink™) did not include the acceleration loop and thus was not a general-purpose simulation.

Although pre-launch testing and in-flight verification were not performed for this particular failure mode, flexible body interaction (excluding slosh) adversely affecting the controller is an unlikely (implausible) cause for the loss of MPL.

#### PROCESS ASSESSMENT

Analyses that were done were carefully executed, but determination of true stability margins would have required a more detailed modeling and characterization incorporating a nonlinear simulation.

### 7.3.9 Zero Velocity Singularity

#### FAILURE MODE DESCRIPTION

This potential failure mode would occur if the lander vertical velocity approaches zero. Under this circumstance, the gravity turn guidance law would command large pitch and yaw turns to compensate for small horizontal velocity errors, leading to an attitude control instability and/or a landing with a large attitude deviation from the vertical.

#### FINDINGS

The MPL team was aware of this singularity condition during the design phase of EDL, and they saw large attitude oscillations in the simulations during testing. Consequently, they introduced a design change to make the guidance loop less sensitive to horizontal velocity errors as the vertical velocity approached its minimum value of 2.4 meters per second. This modification was tested and verified through simulations and analysis to be effective down to a vertical velocity of 1.4 meters per second. Vertical velocity is controlled in a closed-loop way, and as long as the control authority can be regulated down below one Mars g (see Section 7.3.10 below), there is no known mechanism for the vertical velocity to go below 1.4 meters per second.

#### PROCESS ASSESSMENT

Assessment of effects below 1.4 meters per second was not done in sufficient detail.

#### LESSONS LEARNED

The singularity can be removed totally from the system by stopping the gravity turn guidance law and switching to a proportional guidance law at a certain altitude or vertical velocity. In this way, horizontal velocity is still controlled while keeping the bandwidth of this loop constant and independent of vertical velocity.

#### **7.3.10 Minimum Thrust Margin**

##### FAILURE MODE DESCRIPTION

This potential failure mode would occur if the thrust level required to control to constant descent velocity required a lower throttle setting than is available.

##### FINDINGS

All pre-launch simulations show adequate margin; minimum expected throttle setting is comfortably above minimum achievable throttle setting.

#### PROCESS ASSESSMENT

There was a minimum throttle setting command of 25-percent level on all thrusters. More detailed modeling of water hammer and thruster performance shows higher thrust impulse per command setting, meaning less margin above the 25-percent setting. If actual thrust impulse exceeds this model by 10 percent, the system will not be able to set the deceleration low enough to prevent the vertical velocity from being reduced to zero, after which the vehicle would rise instead of fall with respect to the Mars surface. In addition, the control system becomes unstable near zero velocity, and would not be expected to keep the vehicle upright. This is an additional contribution to erosion of control margin.

#### LESSONS LEARNED

Use proportional throttle valve control or ensure that there is ample margin for setting thrust levels as low as required. This may be achieved by changing the strategy for allocation of thrust on time to deceleration vs. attitude control, or by allowing some thrusters to go to 0-percent duty cycle if necessary.

#### **7.3.11 Radar-Heatshield Lockup**

##### FAILURE MODE DESCRIPTION

In this potential failure mode, the Radar locks up on the separated heatshield. This would cause premature parachute separation, and the lander could run out of propellant prior to touchdown and impact the surface with high velocity.

##### FINDINGS

During development, it was assumed that the heatshield would fall to the ground quickly or drift out of the field of view of the Radar. The design includes a search limit (accept only returns from >1220-meter distance) that prevents the Radar from locking onto the heatshield for 25 seconds after

heatshield release. At 25 seconds, when the heatshield is nominally 700 meters away from the lander, this limit is dropped to 40 meters. A February 2000 study by the Radar supplier indicates that there is greater than 9-dB margin below the signal required to lock up on the heatshield at a range of 700 meters.

#### PROCESS ASSESSMENT

Although the process for addressing Radar lockup was properly done from a radar perspective, the actual conditions under which lockup could occur were not adequately understood.

#### LESSONS LEARNED

The maximum distance at which heatshield lockup is possible should be determined. Design the Radar processing algorithm to avoid lockup within this distance.

#### ***Bibliography***

AACS Algorithm: Entry Navigation Kalman Filter, Report Rev. 2, dated 3/11/98, presented on 01/26/00 at LMA.

AACS Algorithm: Radar Commanding, Report Rev. 4, dated 5/25/99, presented on 01/26/00 at LMA.

AAS Algorithm: Radar Processing, Report Rev. 4, dated 06/23/99, presented on 01/26/00 at LMA.

B3. ACS Lander Hardware Description — Kent Hoilman, 01/25/00, viewgraph presentation at LMA.

CG Offset Effect on Landed Location — Bill Willcockson and Jason Wynn, 01/25/00, viewgraph presentation at LMA.

Collection of Action Item Responses from the Dynamics and Control Review Team meeting on 01/25–26/00 at LMA.

Entry Systems — Bill Willcockson, 01/25/00, viewgraph presentation at LMA.

Entry, Descent and Landing (EDL) Overview — John Cuseo, 01/25/00, viewgraph presentation at LMA.

IMU Descent Vibration Environment — Kent Hoilman and Jim Chapel, 01/25/00, graph presented at LMA.

Integrated Propulsion and GN&C System Modeling and Results; Flowtran Propulsion Modeling — Tim Martin, 01/26/00, model presented at LMA.

Lander Entry State File (LESF) — Tom Kelecy, 01/25/00, viewgraph presentation at LMA.

L-GN&C Subsystem Test/Verification — Tom Kelecy, 01/25/00, viewgraph presentation at LMA.

Mars Polar Lander EDL Attitude Determination — Tom Kelecy, 01/25/00, viewgraph presentation at LMA.

Mars Polar Lander EDL Inertial Navigator — Tom Kelecy, 01/25/00, viewgraph presentation at LMA.

Mars Polar Lander Propulsion System Schematic — John Cuseo, 01/25/00, viewgraph presentation at LMA.

Mars Surveyor Program Landing Radar Overview of Flight Tests and GN&C Interfaces — John Cuseo and Bradley Haack, Report AAS 98-067, presented on 01/25/00 at LMA.

MPS Landing Radar Overview — John Cuseo and Dave Cwynar, 01/25/00, viewgraph presentation at LMA.

Radar Test Review — John Cuseo and Brad Haack, 01/25/00, viewgraph presentation at LMA.

Slosh Model — Philip Good, 01/26/00, report presented at LMA.

Surveyor PDS Analysis — via fax Jim Chapel to Bill Ely and Joe Protola, 01/24/00, presented at LMA.

Terminal Descent Phase Overview — John Cuseo, 01/25/00, viewgraph presentation at LMA.

## 7.4 MPL Communications/Command and Data Handling

The Communication/C&DH Review Team charter was to review the telecommunication and command and data handling hardware, software, and system interaction to identify failure modes that could have contributed to an unsuccessful landing and/or failure to establish a telecommunications link. The Review Team met with the MPL team at LMA in Denver, Colorado, on 31 January and 1 February 2000.

The LMA personnel were very open, and non-defensively addressed questions raised by the Review Team. They seemed extremely eager to assist the process of fact-finding and brought in additional expertise as required. Additionally, the Review Team focused on design features that could exacerbate failures, making seemingly recoverable faults non-recoverable. Many of these design features could not be used to explain all the observable data.

The operations team did a good job of scheduling and having appropriate telecommunications coverage. The first 36 hours, in particular, had continuous 70-meter DSN station coverage as well as full-spectrum recorder and open-loop receiver backups. The contingency plans were understood and implemented correctly. The personnel for the first ~20 hours were experienced and knowledgeable about spacecraft communication losses.

This section deals with potential failure modes, findings, and Lessons Learned. In the case of the telecommunications links, more than one event is required to preclude communication with either Earth or MGS; for example, going into safing coupled with a hardware failure. One exception is a landed configuration that would not support a link through any of the antennas.

A separate UHF Subteam looked at the Stanford University testing of the UHF link.

The topic of reviews was discussed with the telecommunications team. An inheritance review was done between the JPL transponder engineers and the LMA telecommunications engineers. The waivers and Problem/Failure Reports (P/FRs) were discussed, including the Red Flag P/FRs. As far as peer reviews, what were called “peer reviews” were presented at the Telecommunications Preliminary and Critical Design Reviews, which were at a high level, as would be expected at a subsystem-level design review. As indicated by LMA, these reviews did include engineers from JPL and from suppliers. Table-top reviews that included experienced engineers from outside the project were not done on all the hardware elements.

### 7.4.1 C&DH Reset During EDL

#### FAILURE MODE DESCRIPTION

The failure or reset of the C&DH during EDL would be mission catastrophic.

#### FINDINGS

The unit was environmentally tested (thermal cycling, random vibration, pyroshock) at the component level. It also was installed on the lander during system-level environmental testing. Live pyrotechnic testing was performed at the system level. There was an Unverified Failure Martin Anomaly Reporting System (MARS) written against the C&DH for a processor reset. It occurred prior to the

Pre-ship Review and was never repeated. This MARS was identified by the MPL Mission Safety and Success Team as a residual risk for EDL.

An SEU event might cause a reset of the processor during EDL. Resources were allocated to analyzing the susceptibility of the processor to SEU events and the probability of a reset occurring during EDL. These analyses were tightly coordinated with JPL and the project used their reliability and radiation experts to calculate the risk to the mission. The results of this study indicated that the probability of a mission-ending reset was less than 0.5 percent.

Extensive testing of the EDL sequences was performed on the spacecraft during ATLO and in the STL prior to and during cruise. Six EDL sequence tests were conducted during ATLO (five on the “A” side and one on the “B” side), and two power profile tests were conducted (also running EDL sequences). All eight EDL runs were completed successfully without processor resets.

Several unplanned C&DH prime swaps occurred in the beginning of the mission. After the cause of this problem was identified, the rest of the mission was flown with the “A” unit of the C&DH prime.

More than 100 EDL sequence runs were conducted in the STL, with more than 55 of them conducted within the last two months before EDL alone. These tests were also completed end to end without any processor resets.

#### PROCESS ASSESSMENT

The component-level environmental test program was a good program. Redundancy is usually included for two reasons: First, it provides a backup so that random failures, which would otherwise shorten a mission can be overcome; second, it increases the availability of the needed functionality in dealing with transient faults during time critical and demanding mission events (such as EDL). The MPL design added redundancy, but did not substantially increase functional availability for dealing with transient faults during critical events.

#### LESSONS LEARNED

Missions that have time-critical phases should include a single fault-tolerant design to processor resets to increase the probability of success.

### **7.4.2 EEPROM Errors After Landing**

#### FAILURE MODE DESCRIPTION

A reset of the C&DH after landing could be mission catastrophic under certain circumstances; e.g., sometime after launch, a stuck bit occurs in the prime string flight computer EEPROM. Since there is no parity nor error detection or correction (EDAC) on the EEPROM, the stuck bit or bits corrupts the flight code in the prime string. After landing, fault protection is re-enabled. A pending fault results in a reset and reload of the flight computer. The corrupted EEPROM is read and begins to execute. It is corrupted in such a way that the heartbeat test in the C&DH Module Interface Card (CMIC) is passed, but then resets again. This process occurs indefinitely with no swap to the alternate string. No MGA antenna deployment occurs and commands never enter the lander.

## FINDINGS

When the EEPROM code was burned, it was CRC checked to insure that the stored file matched the desired file. Following launch, several string swaps occurred that exercised the EEPROM, with no evidence of a stuck bit.

## PROCESS ASSESSMENT

Sometime during flight, a stuck bit in EEPROM could have developed. EEPROM integrity was never verified after launch. A failure of this type could be created. The radiation test data for the EEPROM need to be assessed for its robustness to radiation damage and SEUs.

## LESSONS LEARNED

Flight computer designs should include EDAC on the EEPROMs and should fail the load process if the EDAC indicates a double bit error. Critical memory used to store flight code should be protected from the adverse effects of single stuck bit or SEU faults.

### **7.4.3 CMIC Errors After Landing**

#### FAILURE MODE DESCRIPTION

A reset of the C&DH after landing could be mission catastrophic under certain circumstances; e.g., sometime after launch a bit flip occurs in the CMIC SRAM. This memory is shared by both C&DH strings. The CMIC SRAM is used to store patches to code, which overlay the main program each time the C&DH reloads. There is no parity or EDAC on the CMIC SRAM. After landing, fault protection is re-enabled. A pending fault results in a reset and reload of the flight computer. The corrupted CMIC is read, corrupting the flight code in the prime string. This code begins to execute, resulting in another reset. The CMIC hands control over to the other C&DH string. It powers up and loads its code from EEPROM and then loads the patches from the CMIC. The same corrupted code is transferred into the new string, which then also resets and follows the same path as the previous prime string. This occurs indefinitely, preventing spacecraft control. No MGA antenna deployment occurs and commands never enter the spacecraft.

## FINDINGS

When the CMIC code was updated, it was CRC checked to ensure that the stored file matched the desired file. The CMIC patches and files were controlled by the project change process. Even so, the CMIC file list grew from three at launch to over 100 before EDL. Following launch, several string swaps occurred that exercised the CMIC.

The CMIC SRAM is a single, 1-megabit, radiation-hardened part manufactured by Lockheed Martin Federal Systems. The part has a total dose hardness greater than  $1 \times 10^6$  rad (Si). The lander total dose at the time of landing would have only been a few krads. The part was tested for SEU immunity at LET  $>120$  MeV/mg/cm<sup>2</sup> and found to have an error rate of  $1 \times 10^{-12}$  errors/bit-day. Assuming that all bits of the CMIC SRAM are written to once (effectively) over the length of the mission, this leads to a predicted error rate of  $3.3 \times 10^{-4}$  errors due to SEUs. Thus, stuck bits can only be attributed to hardware failures within the memory elements. When the files are written to the SRAM, the contents are read back and verified against the original file. No errors were detected during cruise during this process. Thus, any failures within the SRAM would have had to occur after the time that the file was placed into memory.



## PROCESS ASSESSMENT

CMIC memory integrity was verified prior to EDL. A failure of this type could occur after the pre-EDL verification and not be detected.

## LESSONS LEARNED

C&DH designs should have EDAC on the CMIC card. Without this, the design is not single-fault tolerant. Critical data should never be stored in a memory where a single fault can incapacitate both strings.

### **7.4.4 Power Controller Unit Fails**

#### FAILURE MODE DESCRIPTION

Any common-mode housekeeping power supply (HKPS) failure that affected both power converters would be mission catastrophic at any time. These two potential failures were examined:

1. The loss of either of the diode OR'ed 15-volt power supply rails. The +15 volt and -15 volt outputs of each HKPS are diode OR'ed and then used to drive some logic. This design allows the failure of either supply without loss of the functions using the diode OR'ed output. However, a failure that causes the loss of the diode OR'ed output would eliminate all the functionality tied to this supply.
2. The A/B SEL (Select) line fails such that each Power Controller Unit (PCU) on the HKPS card alternately powers on and off. The A/B SEL line is a single line driven by an OR gate. Toggle faults on this line would be mission catastrophic.

#### FINDINGS

The PCU design was thoroughly tested pre-launch. Following launch, several C&DH string swaps occurred that exercised the PCU swap logic. After these swaps, no other incidents occurred to test this logic.

#### PROCESS ASSESSMENT

The schematics for the PCU were reviewed to see if the common 15-volt rails represented a significant risk. In each instance where this voltage was used on the PCU, the voltage was not tied directly to any parts, but was resistor isolated from the components that used this voltage. These voltages are also sent "off-board." However, each client for these voltages used fuses to protect these rails from a short at the point of use. The risk from this type of fault seems extremely low.

The second fault introduces a fault condition that was not addressed by the FMECA. A failure of this type would be mission catastrophic, but not very likely.

#### LESSONS LEARNED

Eliminate all common-mode failures from the PCU design. Perform a FMECA that covers both stuck-at and toggle faults. Provide a design that allows both strings of the C&DH to be powered at the same time, but that does not require them to both be powered at the same time.

#### 7.4.5 Landed Orientation Prevents Communication

##### FAILURE MODE DESCRIPTION

In this potential failure mode, X-band and/or UHF link cannot be established due to the landed orientation.

##### *MGA Uplink and Downlink*

The MGA should have been able to support 125 bps commanding up to 6 degrees off boresight in the main beam, and a similar angular range for 2100 bps downlink at a 70-meter station. Neither the onboard sequence nor the subsequent post-EDL commands would have selected a different command rate than 125 bps for the MGA. Thus, any pointing-error greater than 6 degrees is problematical for commanding.

If gyro compassing worked, and the MGA gimbals were functional, then the MGA would have been commanded to track Earth throughout the pass. A gyro-compassing error of greater than 6 degrees would be required to preclude commanding. Commanding via the MGA would also be impossible if the landed azimuth was such that Earth was never inside the gimbal space.

On sol 0, Earth was above 10 degrees elevation for azimuth angles of  $-150$  degrees to  $+75$  degrees (in the nominal landing attitude). Earth elevation peaked at  $\sim 32$  degrees above the horizon. The azimuth and elevation “soft stop” ranges are:  $-138$  degrees  $< AZ < 51.5$  degrees,  $2$  degrees  $< EL < 57$  degrees. The sol 0 Earth geometry is shown in Figure 7-5.

Since the extent of azimuth variation of Earth above 10 degrees is 225 degrees, and the gimbal azimuth range is 189 degrees, Earth is inside the gimbal range for all landed orientations. However, since the MGA is only tracking Earth for a period of up to four hours in a day, or about 60 degrees of azimuth, there is indeed a range of landing orientations that would keep Earth out of the gimbal space during contact periods.

Assuming a good gyro-compassing solution, the four-hour contact periods should effectively add  $\pm 60$  degrees to the 189 degrees azimuth range of motion (because of Mars’s rotation during the tracking period). In other words, the range of azimuth angles not visible during the MGA tracking period is approximately  $360$  degrees  $- 309$  degrees =  $51$  degrees. These would be the azimuth angles directly behind the center of the azimuth gimbal range at  $-43$  degrees, which would put the landing Earth azimuth range for no MGA uplink at approximately  $137$  degrees  $\pm 25$ . This would correspond to a landing azimuth error of  $\sim 180$  degrees  $\pm 25$ . As long as the elevation angle off nominal is less than the specified 16 degrees, the “blind” range above should not be affected too greatly.

For downlink, the “blind” zone is similar if no “touchdown power-on reset (POR)” scenario occurs that would kick off the autonomous Find the Earth (FTE) sequence (see Figure 7-6). Otherwise, the Telecom Subsystem would have been configured for carrier-only downlink for the duration of the sequence, which increases the field of view around the MGA to approximately 30 degrees. In carrier-only mode, a downlink signal would almost certainly have been observed from Earth during the FTE sequence, if the landing azimuth error had been less than 36 degrees (6 degrees FTE minimum “pad” plus 30 degrees field of view).